Analog Integr Circ Sig Process (2013) 75:531–537
DOI 10.1007/s10470-013-0063-5

MIXED SIGNAL LETTER

An 80-V integrated boost converter for piezoelectric actuators in smartphones

Inho Jeon · Hyunseok Nam · Heeyoung Lee · Youngkook Ahn · Jeongjin Roh

Received: 4 July 2012 / Accepted: 13 March 2013 / Published online: 27 March 2013

Abstract A boost converter for piezoelectric actuator driving system in haptic smartphones is proposed and implemented using a 0.35 μm BCDMOS process. The designed boost converter generates extremely high output voltage from a low-voltage battery supply. The boost converter provides stable power for the piezoelectric actuator with the peak-current control technique. The minimum variation of the output ripple variation can be achieved by the designed current-sensing and peak-current control circuits. The supply voltage of the boost converter is 2.7–4.2 V and the maximum output voltage is up to 80 V. The complete piezoelectric actuator driving system consists of a serial interface, SRAM, and signal-shaping logic as well as the boost converter. It also includes the resistor-string digital-to-analog converter and high voltage piezoelectric actuator driver (PZ driver). The fabricated chip size is 2,100 × 2,200 μm, including bonding pads.

Keywords Boost converter · Power converter · Power management

1 Introduction

Recent developments in mobile devices require efficient and application-specific power converters for diverse new applications [1–7]. New developments in haptic technology, which has been implemented in recent mobile devices, is generating great demand for efficient power systems. Especially the haptic technology for the real feeling of touch is progressing with significant importance in market, which generate new requirements in power converters. Diverse researches for applying this haptic technology to mobile devices have been studied [8–13]. To satisfy the life-like details of haptic technology, two main properties are required for an actuator. First, the actuator must have a broad range of frequencies and be functional within a small area. Second, it must have high electrical–kinetic conversion efficiency in mobile devices [11].

Small vibrating motors have been commonly used in mobile devices to realize haptic systems. However, the motor vibrates the entire device and has a limited feedback conversion property. Its slow response is also incompatible with mobile devices that require fast, precise, and diverse feedback for users. To overcome these problems, some research has focused on using piezoelectric actuators for haptic systems. Piezoelectric actuators are smaller in size than vibrating motors, which makes it possible to reduce the critical size of a mobile system. Piezoelectric actuators also have high durability, as well as efficient and diverse actuations that are suitable for various applications [12].

There have been several cases where piezoelectric actuators were applied to a variety of different systems; however, no detailed research relating the circuits of piezoelectric actuators to mobile devices has been published until now. This letter describes the details of piezoelectric actuator driving system and the design of boost converter providing high voltage to the system.

2 Overview of piezoelectric actuator driving system

Figure 1 shows an overall block diagram of a system to drive the piezoelectric actuator. As shown in the figure, when a user's finger comes in contact with the touch

I. Jeon · H. Nam · H. Lee · Y. Ahn · J. Roh (✉)
Department of Electrical Engineering, Hanyang University, Ansan 426-791, Korea
e-mail: jroh@hanyang.ac.kr

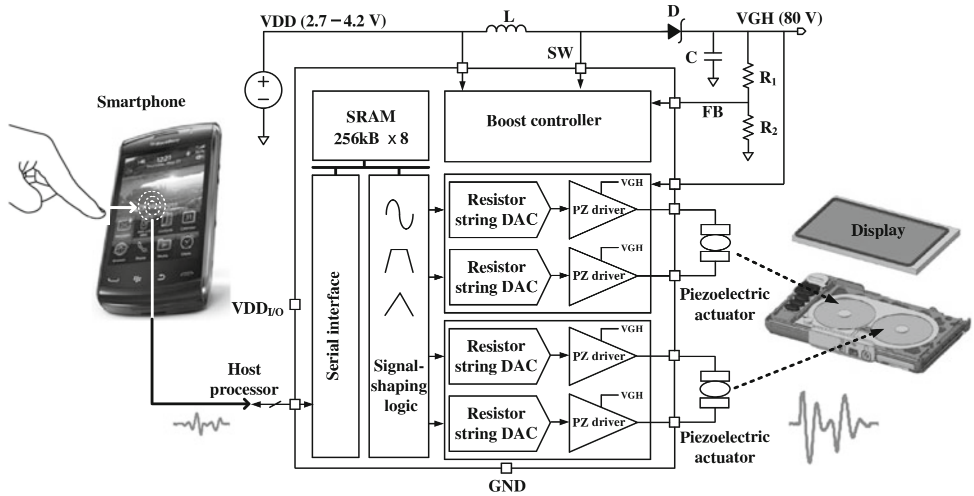

Fig. 1 Piezoelectric actuator driving system for smartphones

screen, different feelings of vibration can be generated by the system. The system receives data from the host processor using a serial interface to operate the piezoelectric actuator driving system. SRAM stores various haptic patterns that operate the piezoelectric actuator and delivers these patterns to the signal-shaping logic. In comparison to delivering patterns directly to the signal-shaping logic via a serial interface, using the stored patterns in SRAM increases the speed of the system by increasing the data transfer rate [13]. Signal-shaping logic uses haptic patterns from the SRAM to alter the frequencies and amplitudes required for the piezoelectric actuator. The haptic patterns are then delivered to the 8-bit resistor string digital-to-analog converter (DAC). The DAC converts the digital waveforms generated by signal-shaping logic to analog voltage and delivers them to the PZ driver. The high voltage PZ driver, which receives power from the boost converter, amplifies the DAC signal and drives the piezoelectric actuator. A reversed phase signal is also applied to the piezoelectric actuator to generate differential voltage for large voltage swing, which in turn results in significant vibration of the actuator.

In order to generate the required high voltage, flyback converters could be another choice for implementation. However, flyback converters use large transformers, which are not suitable for small mobile devices. Therefore, we choose a boost converter to reduce the size of the system in this letter. The designed boost converter generates up to 80 V, and the current-sensing and peak-current control circuits maintain stable and uniform ripple voltage despite the variation of input battery voltage. The boost power converter is implemented by the integrated controller as well as an inductor, a capacitor, a Schottky diode, and feedback resistors as external components.

3 Circuit implementation

Figure 2 shows the PZ driver, which can operate the piezoelectric actuator. The PZ driver is composed of two non-inverting amplifiers and feedback resistors. V_P and V_N are DAC signals and VGH is the output voltage of the boost converter. In general, the piezoelectric actuator can be modeled by a capacitor. In our application system, the capacitance is estimated as 60 nF.

Regarding the effective driving of the piezoelectric actuator, a stronger and vivid vibration can be achieved with differential signals, which are applied to both ends of the piezoelectric actuator as opposed to a single end. Therefore, we use two non-inverting amplifiers to amplify differential signals and apply these to both ends of the actuator. T_S in Fig. 2 is the period of the haptic pattern with maximum frequency of 150 Hz in this system.

The boost converter is based on a burst-mode operation. Figure 3 shows the structure of the designed boost converter. The converter is composed of a power transistor, buffer, comparator, current-sensing circuit, and clock generator. If the output voltage of the boost converter decreases, FB also decreases. Due to the decreased FB, the Comp1 output becomes high and SR latch1 output (EN) also becomes high. During the period when EN is high, the clock (CLK) is delivered to SET and the MN power transistor can be turned on. Once the power transistor turns on, the inductor current increases with a constant slope. When this increasing current reaches a predetermined peak value, the current-sensing circuit senses the current and forces the RST signal to high, which finally turns off the power transistor. This operation is repeated until FB becomes higher than V_{refH}. When FB becomes higher than V_{refH}, Comp2 output becomes high, which makes EN low. As a result, the clock can no longer be delivered to the power transistor.

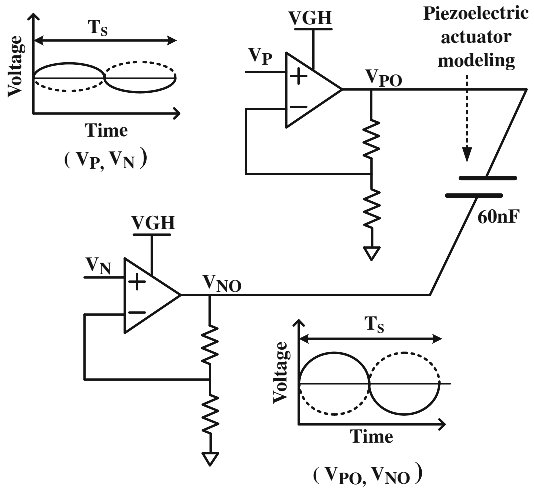

Fig. 2 PZ driver circuit for piezoelectric actuator

Figure 4 shows the designed current-sensing circuit, which is similar to [14]. Start-up and peak-current control circuits are also implemented in order to control the current in the power transistor and limit the peak current. PT1 and PT2 transistors are high voltage MOS transistors. The PT2 transistor copies the current flowing in the power transistor and is 1/800 the size of the power transistor in Fig. 3. D1 and D2 diodes inhibit the high voltage of SW1, and thereby protect the low-voltage transistors (MN1 and MN3) from exceeding the maximum voltage.

When the power transistor and PT1 transistor are turned on, SW and SW1 voltages increase due to the inductor current. Therefore, the gate voltages of MN3 and MN4 transistors also increase. Increased gate voltage, in turn, decreases the drain voltage of the MN4 transistor. The source voltage of the MP4 transistor follows the gate voltage. As a result, V_{SEN} decreases. V_{SEN} is connected to the inverting input of comparator CMP1 and is compared to V_{LT} selected by the analog MUX. V_{LT} is connected to V_{LT1}, V_{LT2}, or V_{LT3}, depending on the operating conditions. Start-up and peak-current control circuits regulate the amount of inductor current in three levels to prohibit a sudden inrush current. The feedback voltage FB, which is the scaled output voltage by resistors, is compared by two comparators, CMP2 and CMP3. Depending on the condition of the output voltage, control logic controls the analog MUX and determines V_{LT}. During the initial start-up operation, the inductor current is regulated by V_{SEN} and V_{LT1}. As the output voltage increases, the inductor peak current is also increased by V_{LT2} and V_{LT3} in turn.

Figure 5 shows the adaptive variation of V_{SEN} and V_{LT} with respect to the supply voltage. As shown in this figure, V_{LT} has to be changed according to the variation of supply voltage. If V_{LT} is fixed to a constant voltage despite the variations in the supply voltage, the output voltage of the boost converter cannot be maintained at a constant level. To solve these problems, V_{LT1}, V_{LT2}, and V_{LT3} used as shown in Fig. 4. V_{LT1}, V_{LT2}, and V_{LT3} are determined by resistors (R_2, R_3, and R_4) and the current source (I_{REF}). The voltages can be expressed as

$$V_{LT1} = VDD - I_{REF}R_2 \tag{1}$$

$$V_{LT2} = VDD - I_{REF}(R_2 + R_3) \tag{2}$$

$$V_{LT3} = VDD - I_{REF}(R_2 + R_3 + R_4) \tag{3}$$

respectively. These voltages have the same amount of variation as the supply voltage, which allows the inductor peak current to be maintained at a constant level. The controlled inductor peak current minimizes the ripple variation in the output voltage.

Fig. 3 Boost converter for PZ driver circuit

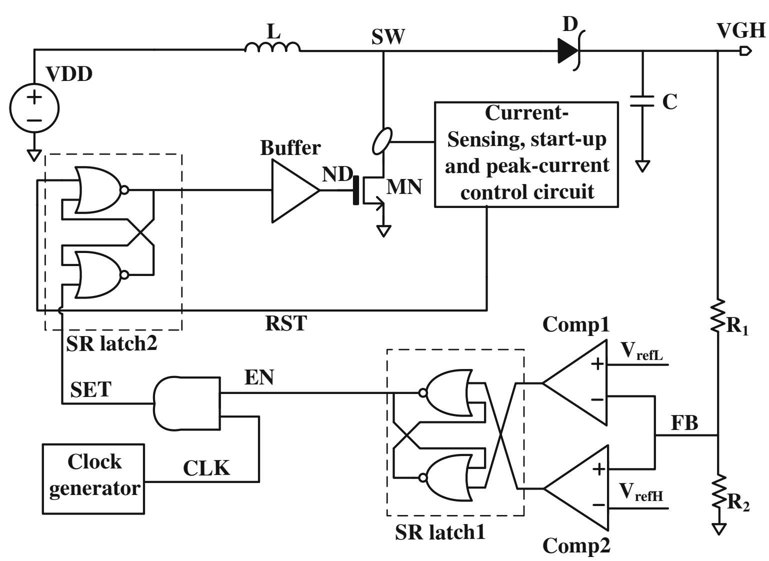

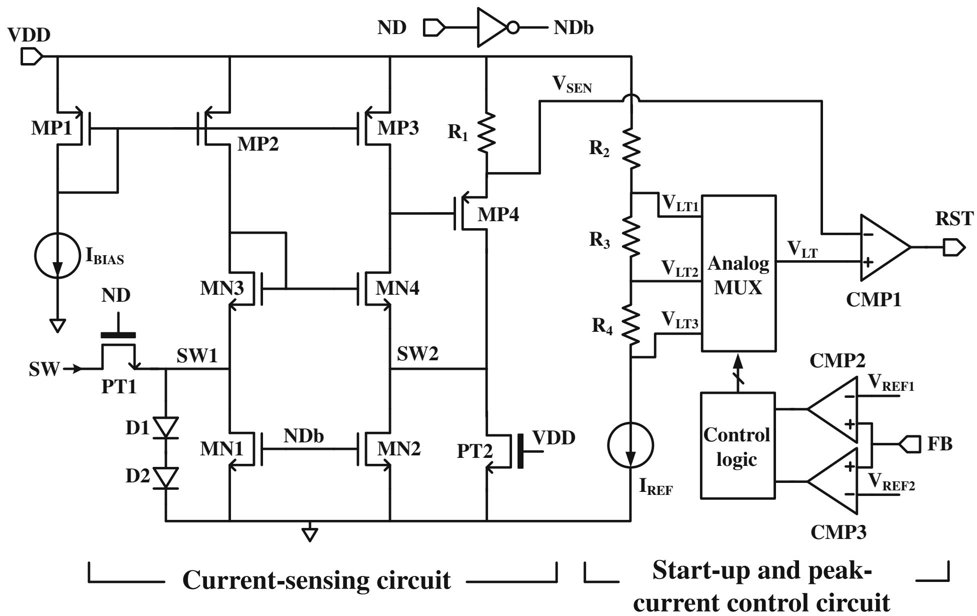

Fig. 4 Current-sensing, start-up and peak-current control circuit

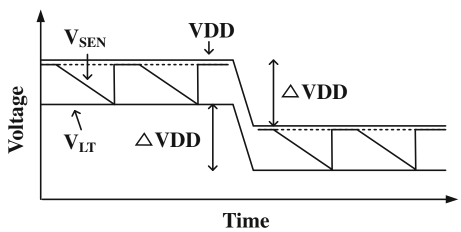

Fig. 5 V_{LT} according to the supply voltage variation

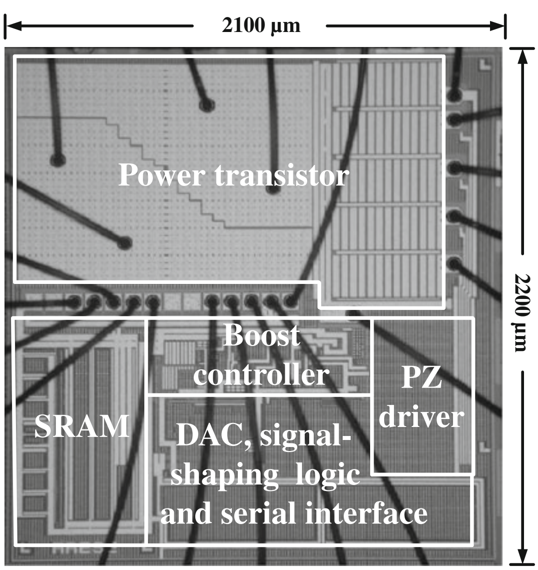

Fig. 6 Chip photograph

4 Experimental results

The piezoelectric actuator driving system was fabricated using the 0.35 μm BCDMOS process. Figure 6 shows the chip photograph. The chip size is 2,100 × 2,200 μm, including bonding pads. The proposed boost converter operates at the supply voltage range of 2.7–4.2 V and generates the maximum output voltage of 80 V. The off-chip inductor and capacitor are 22 μH and 470 nF, respectively. The direct current resistance (DCR) of the inductor and the equivalent series resistance (ESR) of the capacitor are 200 mΩ and 50 mΩ, respectively. Table 1 summarizes the measured performance of the designed system.

Figure 7 shows the start-up waveforms of the boost converter. As seen in the measured waveforms, the boost converter gradually increases the inductor current and the output voltage during the initial operation.

Figure 8 shows the output signal of the PZ drivers along with the output of the boost converter when the input

Table 1 Performance summary

Technology	0.35 μm
Supply voltage (VDD)	2.7–4.2 V
$VDD_{I/O}$	1.8 or 3 V
Output voltage (VGH)	80 V
DAC resolution	8 bit
Clock frequency	68 kHz
Input frequency of PZ driver (max)	150 Hz
SRAM	256 kB × 8
Inductor/DCR	22 μH/200 mΩ
Capacitor/ESR	470 nF/50 mΩ
Efficiency	45 % @ VDD = 4.2 V, VGH = 77 V
Chip size	2,100 × 2,200 μm

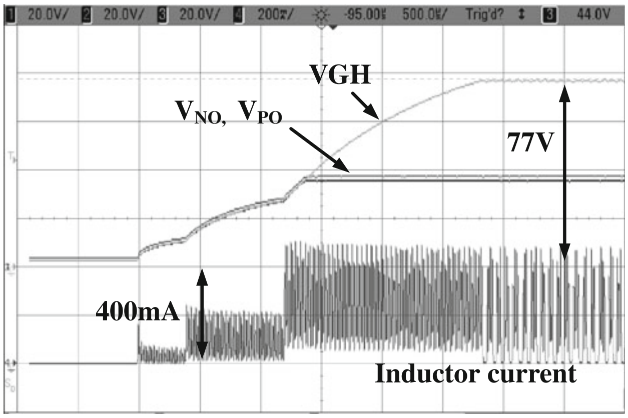

Fig. 7 Measured start-up operation: VDD = 4.2 V, VGH = 77 V, L = 22 μH, C = 470 nF

supply voltage is 2.7 V. The input pattern is a sinusoidal signal with a 70 Hz frequency. Figure 9 shows the waveforms when the supply voltage is 4.2 V. The frequency of the input sinusoidal signal is 90 Hz in this measurement. Figures 10 and 11 show the results when the supply voltages are 2.7 and 4.2 V, and the input patterns are 70 and 120 Hz triangular signals, respectively. As shown in the measurement results, the proposed piezoelectric actuator driving system successfully drives piezoelectric actuators with various input patterns.

5 Conclusion

The boost converter of the single-chip piezoelectric actuator driving system is proposed in this letter for smartphone haptic technology. The designed boost converter generates extremely high output voltage for the piezoelectric actuator, and minimizes the ripple voltage variations by adaptively controlling the inductor peak current. The implemented piezoelectric actuator driving system also integrates the serial interface, a signal-shaping logic, a

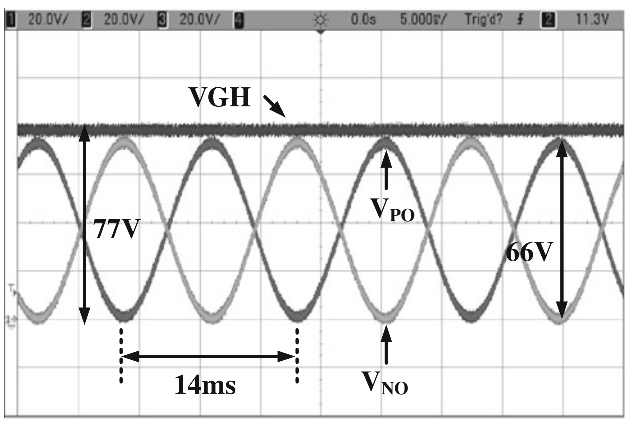

Fig. 8 Measured output voltages of the piezoelectric driver and boost converter: VDD = 2.7 V, VGH = 77 V, L = 22 μH, C = 470 nF, input frequency = 70 Hz (sinusoidal signal)

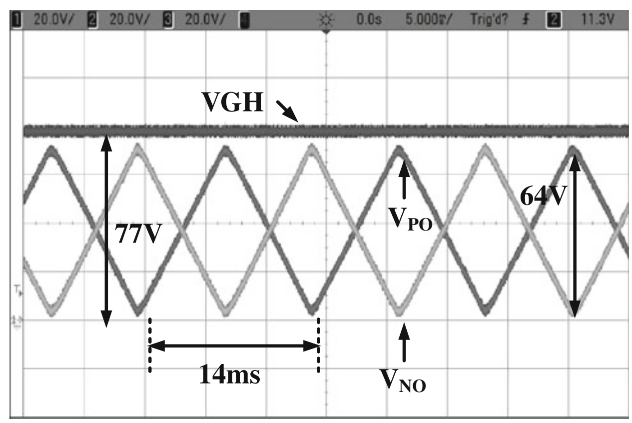

Fig. 10 Measured output voltages of the piezoelectric driver and boost converter: VDD = 2.7 V, VGH = 77 V, L = 22 μH, C = 470 nF, input frequency = 70 Hz (triangular signal)

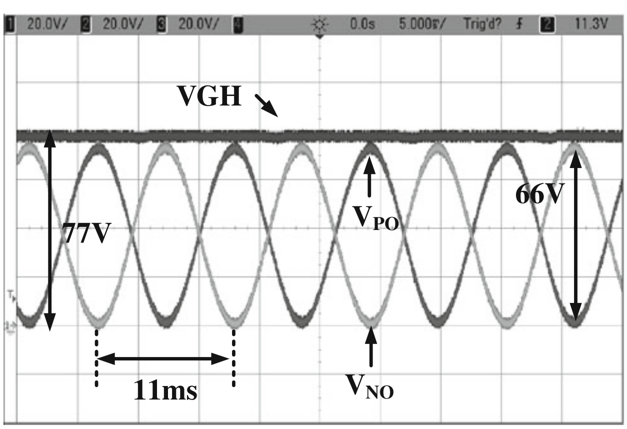

Fig. 9 Measured output voltages of the piezoelectric driver and boost converter: VDD = 4.2 V, VGH = 77 V, L = 22 μH, C = 470 nF, input frequency = 90 Hz (sinusoidal signal)

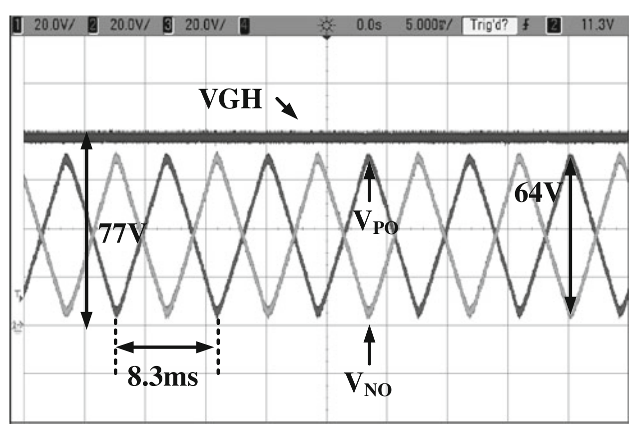

Fig. 11 Measured output voltages of the piezoelectric driver and boost converter: VDD = 4.2 V, VGH = 77 V, L = 22 μH, C = 470 nF, input frequency = 120 Hz (triangular signal)

SRAM block, four 8-bit DACs, and four high voltage amplifiers to drive the piezoelectric actuator. The fabricated chip shows the stable start-up operation, and generates various high voltage waveforms for the piezoelectric actuators.

Acknowledgments This research was supported by the Ministry of Knowledge Economy, Korea, under the University ITRC support program supervised by theNational IT Industry Promotion Agency (NIPA-2013-H0301-13-1007), and supported by the Technology Innovation Program, 10041135, Development of Multi Functional Power Management IC for Smart Mobile Devices funded by the Ministry of Knowledge Economy (MKE, Korea).

References

1. Wens, M., & Steyaert, M. S. J. (2011). A fully integrated CMOS 800-mW four-phase semiconstant ON/OFF-time step-down converter. *IEEE Transactions on Power Electronics, 26*(2), 326–333.
2. Alimadadi, M., Sheikhaei, S., Lemieux, G., Mirabbasi, S., Dunford, W. G., & Palmer, P. R. (2009). A fully integrated 660 MHz low-swing energy-recycling DC–DC converter. *IEEE Transactions on Power Electronics, 24*(6), 1475–1485.
3. Nam, H., Ahn, Y., & Roh, J. (2012). 5-V Buck converter using 3.3-V standard CMOS process with adaptive power transistor driver increasing efficiency and maximum load capacity. *IEEE Transactions on Power Electronics, 27*(1), 463–471.
4. Shangyang, X., Weihong, Q., Miller, G., Wu, T. X., Batarseh, I. (2009). An active compensator scheme for dynamic voltage scaling of voltage regulators. *IEEE Transactions on Power Electronics, 24*(1), 307–311.
5. Barai, M., Sengupta, S., & Biswas, J. (2010). Digital controller for DVS-enabled DC–DC converter. *IEEE Transactions on Power Electronics, 25*(3), 557–573.
6. Weiwei, X., Ye, L., Xiaohan, G., Zhiliang, H., & Killat, D. (2010). A dual-mode single-inductor dual-output switching converter with small ripple. *IEEE Transactions on Power Electronics, 25*(3), 614–623.
7. Huang, M.-H., Tsai, Y.-N., & Chen, K.-H. (2010). Sub-1 V input single-inductor dual-output (SIDO) DC–DC converter with adaptive load-tracking control (ALTC) for single-cell-powered systems. *IEEE Transactions on Power Electronics, 25*(7), 1713–1724.
8. Chen, H.-Y., Park, J., Dai, S., & Tan, H. Z. (2011). Design and evaluation of identifiable key-click signals for mobile devices. *EEE Transactions on Haptics, 44*, 229–241.
9. Yao, H.-Y., Grant, D., & Cruz-Hernandez, J. M. (2011). Perceived vibration strength in mobile devices: The effect of weight and frequency. *IEEE Transactions on Haptics, 3*(1), 56–62.
10. Kaaresoja, T., Anttila, E., & Hoggan, E. (2011). The effect of tactile feedback latency in touchscreen interaction. In: *Proceedings of the IEEE World Haptics Conference (WHC)* (pp. 65–70).
11. Laitinen, P., & Mäenpää, J. (2006). Enabling Mobile Haptic Design: Piezoelectric Actuator Technology Properties in Hand Held Devices. *Proceedings of IEEE International Workshop Haptic Audio Visual Environments and their Applications* (pp. 40–43).
12. Rantala, J., Raisamo, R., Lylykangas, J., Surakka, V., Raisamo, J., Salminen, K., Pakkanen, T., & Hippula, A. (2009). Methods for Presenting Braille Characters on a Mobile Device with a Touchscreen and Tactile Feedback. *IEEE Transactions on Haptics, 2*(1), 28–39.
13. Miribel-Catalàà, P., Montané, E., Lopez-Sanchez, J., Puig-Vidal, M., Bota, S. A., Samitier, J., Simu, U., & Johansson, S. (2002). Smart power integrated circuit for a piezoelectric miniature robot. *Analog Integrated Circuits Signal Process., 33*(2), 191–200.
14. Ma, D., Ki, W.-H., Tsui, C.-Y., & Mok, P. K. T. (2003). Single-inductor multiple-output switching converters with time-multiplexing control in discontinuous conduction mode. *IEEE Journal of Solid-State Circuits, 38*1, 89–100.

Inho Jeon received the B.S. degree in Department of Electronics and Communication Engineering, Hanyang University, Ansan, Korea, in 2012. He is now working toward the M.S. degree in the same department. His research interests include power management circuits and mixed-signal integrated circuits.

Hyunseok Nam received the B.S. degree in electronic and electrical engineering science, Hallym University, Chuncheon, Korea, in 2005. He received the M.S degrees in electrical engineering and computer science, Hanyang University, Ansan, Korea, in 2007, where is currently pursuing the Ph.D. degree. His research interests include power management circuits and mixed-signal integrated circuits.

Heeyoung Lee received the B.S. degree in Department of Electronics and Communication Engineering, Hanyang University, Ansan, Korea, in 2011. He is now working toward the M.S. degree in the same department. His research interests include power management circuits and mixed-signal integrated circuits.

Youngkook Ahn received the B.S. degree in electronic and electrical engineering science, Kyeonsang University, Jinjoo, Korea, in 2006. He received the M.S degrees in electrical engineering and computer science, Hanyang University, Ansan, Korea, in 2009. He is now working toward the Ph.D. degree in the same department. His research interests include power management circuits and mixed-signal integrated circuits.

Jeongjin Roh received the B.S degree in electrical engineering from the Hanyang University, Seoul, Korea, in 1990, the M.S. degree in electrical engineering from the Pennsylvania State University in 1998, and the Ph.D. degree in computer engineering from the University of Texas at Austin in 2001. From 1990 to 1996, he was with the Samsung Electronics, Kiheung, Korea, as a senior circuit designer for several mixed-signal products. From 2000 to 2001, he was with the Intel Corporation, Austin, Texas, as a senior analog designer for delta-sigma data converters. In 2001, he joined the faculty of the Hanyang University, Ansan, Korea. His research interests include oversampled delta-sigma converters and power management circuits.